

Spatial Context Improves the Integration of Text with Remote Sensing for Mapping Environmental Variables

Valerie Zermatten^{a,*}, Chiara Vanalli^a, Gencer Sumbul^a, Diego Marcos^b, Devis Tuia^a

^a*ECEO, Ecole Polytechnique Fédérale de Lausanne (EPFL), 1951 Sion, Switzerland.*

^b*INRIA, University of Montpellier, Montpellier 34090, France.*

Abstract

1. Recent developments in natural language processing highlight text as an emerging data source for ecology. Textual resources carry unique information that can be used in complementarity with geospatial data sources, such as remote sensing imagery, thus providing insights at the local scale into environmental conditions and properties hidden from more traditional data sources.

2. Leveraging textual information in a spatial context presents several challenges. First, the contribution of textual data remains poorly defined in an ecological context, and it is unclear for which tasks it should be incorporated. Unlike ubiquitous satellite imagery or environmental covariates, the availability of textual data is sparse and irregular; its integration with geospatial data is not straightforward. Moreover, text descriptions, typically those about environmental conditions, can be relevant for areas of variable size, sometimes over vast regions, introducing a high variability in the size of the spatial context to be integrated.

3. In response to these challenges, this work proposes an attention-based approach that combines aerial imagery and geolocated text within a spatial neighbourhood, i.e. integrating contributions from several nearby observations. Our approach combines vision and text representations with a geolocation encoding, allowing it to explicitly take into account the spatial structure of the original observations. The attention-based module dynamically selects spatial neighbours that are useful for predictive tasks, enabling the processing of a flexible range of inputs, with a spatial context of dynamic size.

4. The proposed approach is applied to the EcoWikiRS dataset, which combines high-resolution aerial imagery with sentences extracted from Wikipedia describing local environmental conditions across Switzerland. Our model is evaluated on the task of predicting 103 environmental variables from the SWECO25 data cube. Our approach consistently outperforms single-location or unimodal, i.e. image-only or text-only, baselines. When analysing variables by thematic groups, results show a significant improvement in performance for climatic,

*Corresponding Author: [valerie.zermatten\[at\]epfl.ch](mailto:valerie.zermatten@epfl.ch)

edaphic, population and land use/land cover variables, underscoring the benefit of including the spatial context when combining text and image data. Overall, our findings demonstrate an advantage of injecting knowledge through text when spatially modelling environmental variables with remote sensing imagery.

Keywords: Remote Sensing, Spatial Context, Spatial Interpolation, Switzerland, Text, Vision-Language Models, Wikipedia.

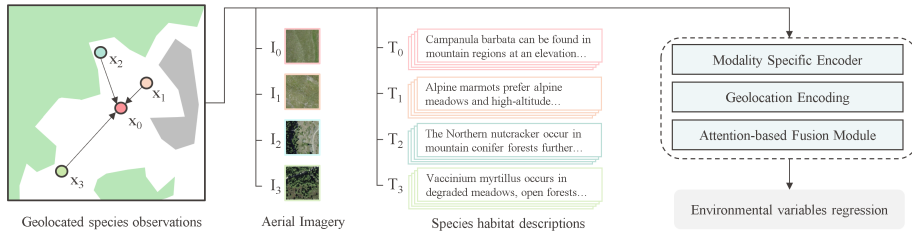


Figure 1: We study how to effectively combine remote sensing images and geolocated text for predicting a variety of environmental variables with a single deep learning model. For a location of interest (x_0), we use the geolocation of species observations in crowdsourcing platforms as a way to introduce geolocated text: We combine aerial images (I_0 to I_3) with text describing the species habitat extracted from its Wikipedia article (T_0 to T_3) and encode them with pretrained vision and text encoders, respectively. We incorporate several spatial neighbours that are in the vicinity of the location of interest and keep the spatial organisation of the observation by encoding geolocation (x_0 to x_3). We fuse all the textual and visual inputs through an attention-based fusion module that dynamically selects which neighbours are useful.

1. Introduction

Recent advances in machine learning applied to remote sensing images have enabled large-scale, cost-effective monitoring of the natural environment, supporting a variety of applications such as terrestrial plant diversity mapping (Wang and Gamon, 2019), canopy height estimation (Lang et al., 2023), species distribution modelling (Deneu et al., 2022), offshore industrial activities mapping (Paolo et al., 2024), population estimation (Metzger et al., 2022), bioclimatic variables regression (Waltari et al., 2014) or water quality monitoring (Sun et al., 2022).

The whole complexity of natural environments is rarely captured by a single data source. The use of heterogeneous data sources is often essential for a comprehensive understanding of ecological dynamics, with approaches that combine remote sensing with additional sources such as bioclimatic variables, in situ observations or laboratory measurements (Cavender-Bares et al., 2022; Miao et al., 2024; Liu et al., 2024; Abdelwahed et al., 2025; Zbinden et al., 2025). These heterogeneous data sources provide complementary perspectives on natural processes, each contributing unique information revealing details possibly

not available in other sources. Integration of heterogeneous data sources can be challenging, particularly for those that are not available regularly, i.e. following a sparse sampling process, but recent approaches show first successes for this type of multimodal logic.

A new promising ecological data modality is text. The integration of textual information in environmental modelling pipelines holds promises and could bring significant contributions to applications at the intersection of natural language processing and ecology (Xue and Zhu, 2025; Miao et al., 2024). Of particular interest is the possibility of injecting knowledge through text into machine learning models. Automatic methods to process text enable information retrieval and structuring that would otherwise require several time-consuming, manual pre-processing steps (Castro et al., 2024). Various textual resources have been exploited to obtain specialised knowledge for a variety of applications, such as collecting plant traits systematically from the web (Marcos et al., 2025; Domazetoski et al., 2023; Paz-Argaman et al., 2020), monitoring illegal wildlife trade from online trade platforms (Stringham et al., 2021), or quantifying temporal ecological patterns from social media posts (Hart et al., 2018; Miłodrowski et al., 2025). The emergence of Large Language Models (LLMs) has also facilitated the filtering and rephrasing of the information coming from text, enabling an easier integration into machine learning models (Hamilton et al., 2024; Wen et al., 2025; Castro et al., 2024). Given the risks of LLMs to produce hallucinations and to introduce spurious biases in modelling pipelines, the relevance and correctness of the collected text content have also been assessed in recent works (Castro et al., 2024; Miao et al., 2024; Dorm et al., 2025).

The integration of text with other modalities has been significantly improved with Vision-Language Models (VLMs). CLIP (Radford et al., 2021), one well known VLMs, leverages the rich language semantics of image-text pairs extracted from the web for predicting image labels in zero-shot settings, i.e. predicting an image label without being explicitly trained for it. CLIP-like models have been widely leveraged: On the one hand, language semantics facilitate the transferability of annotations for real-world applications by harmonising different nomenclatures. On the other hand, the use of free-form text can be used as a supervision to introduce human expertise in a flexible manner in visual recognition tasks. For instance, WildCLIP (Gabeff et al., 2024) adapts the CLIP model to retrieve scenic, behavioural, and species attributes from camera trap images with user-defined queries expressed with language. BioCLIP (Gu et al., 2025; Stevens et al., 2024) leverages the natural hierarchy between species taxonomic names to improve fine-grained species recognition. INQUIRE (Vendrow et al., 2024) introduces a challenging text-to-image retrieval benchmark with textual descriptions that reflect real-world scientific queries, encouraging the development of retrieval systems that can support ecological and biodiversity research.

To study ecological geospatial processes, texts need to be associated with a geographic location. Geotagged social media posts (Häberle et al., 2022; Sathianarayanan et al., 2024; Yang et al., 2022), volunteered geographic in-

formation (VGI) such as OpenStreetMap (Wang et al., 2024; de Arruda et al., 2024; Fonte et al., 2018), or web content associated with geographic coordinates (Uzkent et al., 2019) are frequently used as a mean to associate a text with geographic coordinates. Alternatively, some texts can be associated with a geolocation by exploiting information explicitly present in the text (e.g. addresses, toponyms), or a relative description of the place, and also by identifying specific language features, such as dialects and idioms, to infer the location of the speaker (Derungs and Purves, 2014; Stock et al., 2022).

In ecology, a creative way to attach text to geographic coordinates is to exploit geo-tagged wildlife observations from crowd-sourcing platforms, where geolocations are paired with textual descriptions of the species (Daroya et al., 2025; Hamilton et al., 2024; Zermatten et al., 2025; Lange et al., 2025). Species descriptions, such as those coming from Wikipedia, provide valuable details on the ecological preferences of species, with clues on land cover, soil properties, relationship to humans, climatic conditions, distribution range and co-occurrence with other species. Thus, species observations are a rich source of information for ecology, since they reflect the local natural conditions around each observation, and are available globally. Combined with other resources, they have shown to be beneficial for several geospatial tasks. For instance, integrating text from Wikipedia in WildSAT (Daroya et al., 2025) has improved the recognition performance on satellite imagery at a global scale. The authors of EcoWikiRS (Zermatten et al., 2025) show that sentences describing local environmental conditions contribute to a better identification of fine-grained ecosystems and their characteristics from aerial imagery, while in (Hamilton et al., 2024), habitat or range descriptions enhance the accuracy of species distribution maps for species with few observations.

The use of text within geospatial ecological modelling is promising, yet faces significant obstacles. First, text is not a point measurement and exhibits geolocation ambiguity. Some texts, such as those describing natural features, are often valid over broad regions, and it is not always possible to link them to a specific area, such as municipal boundaries or standard land cover polygons. This geolocation ambiguity reflects not only the precision with which an ecological text is geolocated, but also the range for which a text is considered a valid descriptor. Instead of assigning text to a specific point or area, results can be shared as a probability distribution rather than a pair of coordinates (Dufour et al., 2025). Second is geographic biases. A large share of textual resources relies on crowd-sourced data, which are socio-economically and geographically biased towards the global north and populated places, while species observations are biased towards charismatic taxa (Wolf et al., 2022). Geo-referenced text often exhibits an uneven spatial distribution or an imprecise geolocation, resulting in noisy and inconsistently spread data. Such sparsity of textual data makes integration with continuous data (e.g., imagery, environmental rasters, etc.) challenging and demands specific integration methodologies.

The irregularity and sparsity of text data make it difficult to exploit methods relying on a fixed neighbourhood and tend to lead to inconsistent esti-

mates. Transformations to continuous representations (interpolation) or density are often used instead. Methods relying on geostatistics have been developed to explicitly use spatial dependencies in interpolation: Kriging (Cressie, 1990) exploits spatial dependencies to characterise the range of autocorrelation and predict values at unobserved locations, and is widely used in disciplines such as meteorology, e.g. for snow depth prediction or temperature estimation. Geographically Weighted Regression (GWR) (Fotheringham et al., 2009) incorporates spatial dependencies by fitting local regression parameters, in which nearby samples exert greater influence on parameter estimates, and has been used to estimate the net primary production of forest ecosystems (Wang et al., 2005). Graph Neural Networks (GNNs) learn relevant geographic context by optimally weighting the spatial relationships across training samples. Recent works combine geostatistics with deep learning methods: Kriging Convolutional Networks (Appleby et al., 2020) merge the advantages of GNNs and Kriging by directly combining neighbours to make spatial predictions, for example, in bird count modelling or for estimating precipitation distribution. Similarly, Deep Kriging Neural Networks (Chen et al., 2024) include a deep-learning-based spatial encoder and a Kriging-based decoder and obtain a high performance for modelling meteorological data in the continental United States.

Location encoding methods have also been explored to integrate geospatial context (Klemmer et al., 2025b). They encode geographic coordinates into a high-dimensional vector, or location embedding, that is directly usable by machine learning models. Numerous studies have shown the benefit of location encoding to improve model performance in many geospatial applications, ranging from species distribution modelling, fine-grained species recognition, or climate variables estimation (Mac Aodha et al., 2019; Cole et al., 2023; Chu et al., 2019; Rufswurm et al., 2024; Lange et al., 2025). Embeddings that capture the local characteristics of a place have also been built upon visual representations from satellite (Klemmer et al., 2025a) or ground-level imagery (Mai et al., 2023).

In this work, we study how to synergise text information from crowdsourced resources with very high-resolution remote sensing imagery to regress environmental and climatic variables. Xue and Zhu (2025) recently highlighted the potential of such synergy, which enables the prediction of continuous, real-valued environmental or geophysical variables (e.g. forest height, climatic variables, hydrology, population estimate). However, the absence of dedicated benchmarks and the challenge of combining discrete (text) and continuous (RS imagery or other grid-like data) variables were raised as core obstacles for the development of this field. Tackling these issues, we focus on three aspects: the contribution of text, strategies to integrate it, and a dataset for evaluation.

- First, we investigate whether text provides complementary information to remote sensing data for mapping environmental variables. To evaluate this both quantitatively and qualitatively, we compare the contributions of text and RS imagery in a multiple regression task predicting 103 environmental variables simultaneously. The variables are grouped into 7 groups:

vegetation, climate, geology, hydrology, soil (edaphic), population, and land use/land cover.

- Second, we address the challenge of combining sparsely geolocalised text with continuous RS imagery by proposing an attention-based architecture that explicitly takes into account the geospatial context of the observations. We propose to learn from a spatial context that goes beyond the strict location of a point of interest and leverages nearby observations, therefore improving robustness against noisy or sparse data. Practically, this is implemented as a form of spatial smoothing, by combining data at the point of interest with observations from the nearest neighbours in terms of geographical distance. We also preserve the spatial arrangement between samples with location embeddings. The attention-based architecture dynamically selects the most relevant neighbours by including a notion of geographic distance, while dynamically learning the range of the spatial context that is useful.
- We test our approach on the EcoWikiRS dataset (Zermatten et al., 2025) composed of aerial imagery over the Swiss territory and geo-referenced text extracted from Wikipedia that describes the local environmental context. As target, we use 103 variables from SWECO25 (Külling et al., 2024), a raster database for ecological research, extracted at each location present in the EcoWikiRS dataset. We release this evaluation dataset, addressing the current lack of standardised comparison for VLMs in spatial regression tasks (Xue and Zhu, 2025).

We believe that the proposed approach sheds light on the role of text for geospatial regressions and has the potential to address challenges related to the incorporation of sparse texts with continuous RS imagery. Moreover, the approach is broadly transferable to other domains and tasks in ecology that integrate spatially geolocated textual information.

2. Materials and Methods

The proposed approach integrates geolocated text and aerial images from nearby locations to predict 103 environmental variables using a multiple regression approach. Our multimodal approach is based on a vision-language transformer model that is able to ingest both remote sensing images and textual descriptions. The overall model architecture is shown in Fig. 2. We adopted a modular architecture that consists of an image encoder, a text encoder, a location encoder, and an attention-based fusion module. Similar to a graph-based approach or to GWR, the model learns to estimate a different weight for each nearby observation at each location of interest through its attention mechanism.

2.1. Preliminaries

We consider a dataset composed of N geolocated samples with the following elements: the location $x_i \in \mathbb{R}^2$ is a GPS coordinate; $I_i \in \mathbb{R}^{3 \times h \times w}$ is a remote

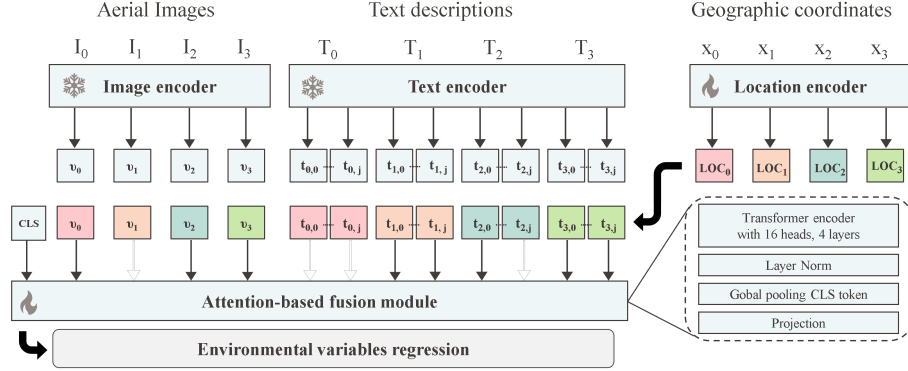


Figure 2: The proposed model architecture is illustrated with a spatial context of 3 nearest neighbours ($k=3$), with images, text and their respective geolocations as inputs. The pre-trained encoders for image and text are frozen, while the location encoder and the attention-based fusion module are trained. Random token masking (dashed arrows) is applied on the generated visual (v_i) and textual ($t_{i,j}$) embeddings after the fusion with the location encoding (LOC_i). The final predictions are derived from the classification token (CLS) at the output of the attention-based fusion module. Colours denote distinct geographic locations.

sensing image of location x_i with RGB bands; $T_i = \{s_{i,0}, \dots, s_{i,j}\}$ is the set of j text sentences associated with location x_i ; and $y_i \in \mathbb{R}^m$ is the set of target numerical environmental variables, while m denotes the number of environmental variables to be predicted.

For each location x_i , we compile the list of $k \in \mathbb{N}$ nearest samples (or k nearest neighbours, kNN). The neighbours are defined in terms of Euclidean distance between the respective geographic coordinates, sorted by increasing distance, while $k = 0$ denotes the index of the location of interest. Thus, a training sample p_i is made of $k + 1$ geographic coordinates, i.e. one for the location of interest and k for its NN, and, following the same logic, $k + 1$ remote sensing images and $k + 1$ sets of sentences. Thus, each training sample integrating context from k neighbours can be written as follows:

$$p_i = \{x_{i,0}, \dots, x_{i,k}, I_{i,0}, \dots, I_{i,k}, T_{i,0}, \dots, T_{i,k}\}$$

The proposed approach aims at learning a model f that estimates the environmental variables y_* for a new location x_* , as $\hat{y}_* = f(p_*)$

2.2. Text and image encoding

Given a training location p_i , a pretrained visual encoder f_v encodes the $k + 1$ remote sensing images into $k + 1$ visual embeddings $(v_i)_{i=0}^k$ with $v_i \in \mathbb{R}^d$. For each location, a number j of sentences is then selected for encoding. We found empirically that selecting the top- j sentences per location by computing the cosine similarity with the visual embeddings using a pretrained VLM is the most effective way to integrate text information. More details are available in Section 3.3. The selected sentences are then fed to a tokeniser and to a

pretrained text encoder f_t , producing $j(k+1)$ textual embeddings $(t_i)_{i=0}^{j(k+1)}$ with $t_i \in \mathbb{R}^d$.

2.3. Location encoding

We encode the spatial structure of each textual and visual embedding by combining it with a geolocation encoding based on their geographic coordinates (LOC in Fig. 2). We compare several approaches, while the results are discussed in Section 3.3.2:

- **None:** No geolocation information is provided.
- **Rank:** We encode the rank of nearest neighbours, i.e. the k in the kNN, similarly to NLP approaches that encode the position of a token in a sequence. For that, we use a 512 dimensional 1D sinusoidal encoding, similarly to the Transformer positional encoding (Vaswani et al., 2017). Then, the embeddings are concatenated with the text and visual features and merged through a fully connected (FC) layer.
- **Learnable:** Similarly to *rank* above, we encode the rank of nearest neighbours for both text and image embeddings, but with learnable embeddings. The embeddings are initialized with a uniform distribution between $[\frac{-1}{h_{dim}^{1/2}}, \frac{1}{h_{dim}^{1/2}}]$ and summed with the corresponding vision and text embeddings.
- **Coordinates:** We encode the geographic coordinates for each location with a 2D sinusoidal multi-scale encoding, similarly to the “grid” approach in Mai et al. (2020). We scale the geographic coordinates to a relative scale in the range $[0, 1]$ based on the min-max coordinates of the study area. We encode each coordinate, i.e. North and East, separately with $h_{dim}/2 = 256$ dimensions. We concatenate them together with their corresponding text or visual embeddings, and finally combine them through a FC layer.
- **Distance:** We encode the relative position of the nearest neighbours with the Euclidean distance in meters from the origin to the target nearest neighbour with 1D sinusoidal encoding with $h_{dim} = 512$ dimensions up to a maximum distance of 10'000 m. We concatenate the distance embeddings with their corresponding text or visual embeddings and combine them through a FC layer.
- **Polar:** Mai et al. (2020) showed that using polar coordinates outperforms grid-like approaches. We combine the Euclidean distance from the origin to the target nearest neighbour with the angle between the positive x-axis and the vector pointing from the origin to the nearest neighbour. We use sinusoidal functions to encode both the distance and the angle, similarly to the “polar” approach from Mai et al. (2020). We concatenate the distance, the angle and the features embedding together and combine them through a 1-layer MLP.

After encoding the location for all inputs, each text and visual embedding can be considered as an input token without specific order, since the relative location to the origin is preserved, thanks to the location embeddings.

2.4. Multi-modal fusion with the attention-based module

Once all inputs have been encoded into a common embedding space, fusion can be performed. The fusion module is composed of a transformer encoder, a layer-normalisation layer, a global pooling layer on the global classification (CLS) token and a projection layer that leads to the final model predictions. The attention mechanisms in the transformer encoder enable the fusion of the multi-modal tokens. The motivation behind this design is that the attention mechanism enables to weight dynamically spatial neighbours, emphasising the most informative neighbours, while ignoring distant or irrelevant ones, thereby learning a context-aware spatial representation.

2.5. Dataset

This section describes the datasets used in our experiments.

2.5.1. EcoWikiRS

The EcoWikiRS (Zermatten et al., 2025) dataset contains over 90'000 text-image pairs, combining high-resolution RGB aerial imagery from Switzerland with sentences from Wikipedia describing the habitat of a species observed at the location of the images. The species habitat description and aerial images have been paired together by using the geolocation of crowd-sourced species observations from the Global Biodiversity Information Facility (GBIF)¹. A specificity of this dataset is that most images are paired with more than one sentence, since several sentences are usually extracted from each Wikipedia article, depending on the number of species found and the length of the corresponding Wikipedia article. The dataset is split into train, validation and test following a spatial block split, with a block size of roughly 20 km, and nearest neighbours are sampled only within the same split. This avoids performance inflation due to spatially autocorrelated training and test samples, when using a random split with geolocated observations (Kattenborn et al., 2022).

2.5.2. SWECO25

We assess the contribution of each modality in the EcoWikiRS dataset by evaluating its capacity to predict environmental variables. For this task, we use the SWECO25 (Külling et al., 2024) dataset, a data cube of more than 5'000 environmental rasters at 25m spatial resolution covering Switzerland. For each location in EcoWikiRS, we extract average values covering the surface of the input image (100 × 100m) for 103 selected SWECO25 variables. We standardise the numerical values across the training set for zero-mean and unit

¹<https://www.gbif.org/>

variance. The Supplementary Section 4.3 provides more details on the selection, preprocessing and individual description of the SWECO25 variables. The 103 variables are grouped into seven thematic groups, following the groups formed in the SWECO25 dataset. We recall here a short description of each group, and more details are available in the Suppl. Table 1:

- Bioclimatic: Bioclimatic variables from WordClim.
- Geologic: Subsoil classified according to lithological criteria.
- Hydrological: Distance to the hydrological network and ecomorphological state of rivers.
- Edaphic: Ecological indicator values for soil properties and nitrogen and phosphorus loads.
- Land use and cover: Land-use and cover classification.
- Population: Human population density and distance to transportation network.
- Vegetation: Vegetation height and dominant leaf type.

2.6. Experimental setup

The model is trained for 100 epochs to minimise a mean squared error (MSE) loss, a standard loss for regression, by using the AdamW optimiser (Loshchilov and Hutter, 2019) with the initial learning rate of $1e^{-4}$ and the mini-batch size of 256. We use the pretrained text and vision encoders from SkyCLIP-ViT-B (Wang et al., 2024), following its effectiveness on the EcoWikiRS dataset (Zermatten et al., 2025). We also explored the use of a general vision encoder for encoding the image and a pretrained LLM to produce text representations, but found empirically that the alignment learned with contrastive learning between text and image features, as in SkyCLIP, provides a more accurate multi-modal fusion in our approach. We empirically observed that fine-tuning or not the visual and textual encoders does not lead to significant performance differences; thus, we keep both of them frozen.

During training, random token masking is applied on the visual and textual tokens, with the probability of 30%, to reduce overfitting and increase model robustness to varying NN distances. We use the *habitat* sentences from the EcoWikiRS data, i.e. sentences relative to the habitat section of the article only, since they were shown to perform best in Zermatten et al. (2025). We use the four sentences with the highest cosine similarity to the image in the SkyCLIP latent space, i.e. top- j sentence with $j = 4$. If fewer than four sentences are available, sentences are chosen with replacement. If not mentioned otherwise, a *polar* location encoding is applied. We evaluated the regression of environmental variables with the Pearson correlation coefficient (R^2).

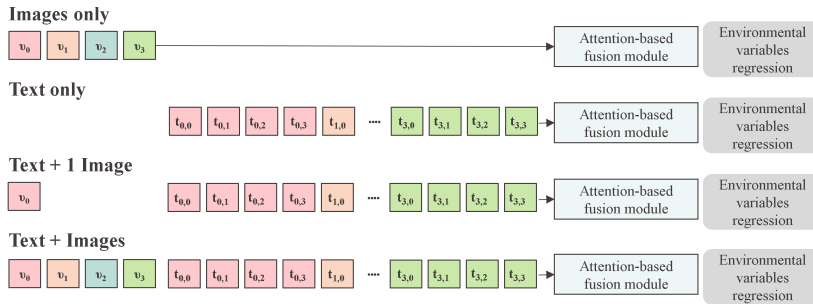


Figure 3: Different experimental settings used to explore various modality combinations, using three spatial neighbours ($k=3$) and four sentences per location ($j = 4$). Colours denote distinct geographic locations.

3. Results

The performance of the proposed approach is assessed against single-location and single-modality baselines in Section 3.1. Then, an analysis by thematic group of environmental variables is presented in Section 3.2, which highlights the different contributions of text and images for specific environmental variables. Finally, Section 3.3 analyses the contributions of the various model components to the overall performance, such as text inputs (number of sentences, text selection) and location encoding approaches.

3.1. Combining text and images in a spatial context

We exploit the architectural flexibility of our model for systematically testing how different modalities and different numbers of neighbours affect the predictive performance. Specifically, we compare several settings using data from a single location (without spatial context) versus several nearest neighbours (with spatial context) and evaluate the effect of combining text and images. All settings are shown in Fig. 3. The “Text only” and the “Images only” settings use exclusively one modality, whereas both modalities are mixed together in the “Text + Images” experiment. We also observe the contribution of a single image location, with text (“Text + 1 Image”), since adding a single image at the location of interest provides a significant contribution in many cases.

Fig. 4 shows the mean coefficient of correlation R^2 on the EcoWikiRS test set for predicting the environmental variables with the standard deviation over five random seeds. The best performances are obtained when combining text and images, both with spatial context, with an R^2 score of 0.50 (“Text + Images”) or without spatial context with an R^2 score of 0.43 (“Text + 1 Image”, “Text + Images”, i.e. equivalent setting without NN). This confirms that incorporating text with images brings complementary information, and combining them is key to reaching the highest performance. The comparison between “Text only” and “Image only” models demonstrates that images carry richer information for the considered tasks, both with or without spatial context. This is confirmed with

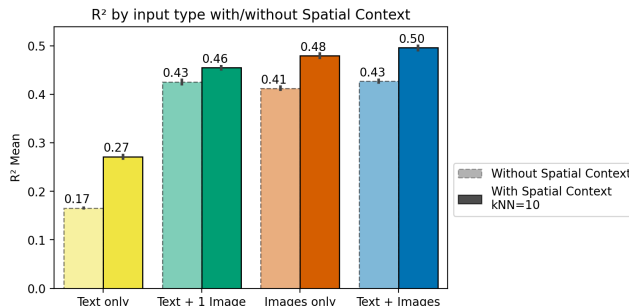


Figure 4: Mean coefficient of correlation R^2 on the EcoWikiRS test set for predicting SWECO25 variables, with images, text or their combination as input, comparing with or without spatial context ($k=10$). The black line over each bar indicates the standard deviation across five random seeds.

the “Text + 1 Image” setting, which shows that the corresponding RS image at origin carries an important share of the information, and offers a significant boost in performance compared to the “Text only” setting. Integrating spatial context ($k = 10$) consistently improves predictive performance across all settings, compared to using data from a single location. The “Text only” approach benefits the most from the integration of context, with its performance rising from 0.17 to 0.27 (+58%).

Fig. 5 illustrates how the number of nearest neighbours affects the accuracy metrics. Performance increases steadily up to 10 NN, after which it stagnates or even drops for all models. Including distant neighbours yields no meaningful performance gain while increasing computational cost, arguing for a conservative approach to data integration. This behaviour is better understood when looking at the Suppl. Figs 12-13, which illustrates the mean distance to NN, and the spatial autocorrelation between input observations, measured as the feature similarity as a function of distance. Higher similarity between features occurs up to a distance of 1’000 m for visual embeddings, and 700 m for the text ones, on average, which is close to the average distance of the 10th NN, which equals 880 m. This suggests that the spatial attention mechanism implicitly learns geospatial statistics and effectively uses them to weight input features.

Fig. 6 confirms this hypothesis and shows the attention for all visual and text tokens as a function of distance, in the test set. The attention score is computed as the logarithm of the maximum attention score across all transformer encoder layers for the best “Text + Images” model and plotted as distance bins of 100 m. Both modalities exhibit their highest attention values at short distances, which then monotonically decrease up to a distance of about 1’000 m. The visual tokens exhibit, overall, a higher attention score compared to the text tokens.

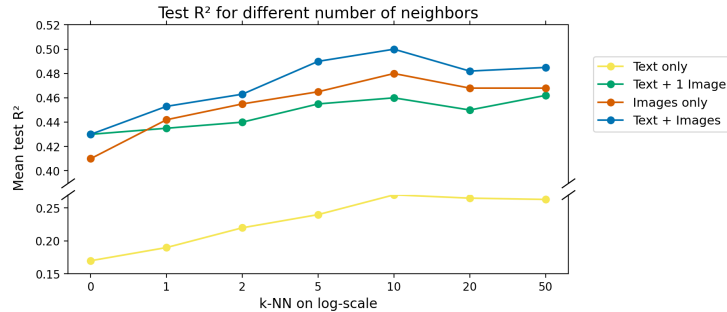


Figure 5: Mean coefficient of correlation R^2 for predicting SWECO25 variables on the EcoWikiRS test set, when adding incrementally more neighbours. The axis is discontinuous between 0.27 and 0.40 for clarity of presentation.

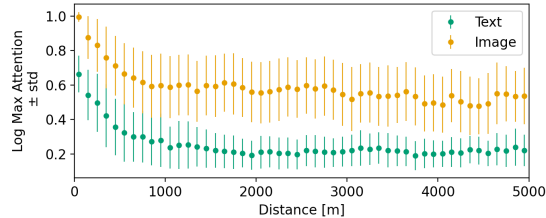


Figure 6: Attention visualisations for the text and image model on the EcoWikiRS test set. Attention values are log-maximum scores taken across all layers and scaled to $[0, 1]$, and they are represented as means and standard deviations, split per distance bins of 100m.

3.2. Specific contribution of text and images for different types of environmental variables

Fig. 7 shows the comparison of the regression performances of our best model, i.e. “Text + Images”, with or without spatial context, for the SWECO25 variables grouped into seven thematic groups. Additional scatter plots of predicted values against SWECO25 values are presented in the Suppl. Fig. 14 to give more insight into performance at the variable level.

For all the thematic groups, a gain in performance is obtained when adding spatial context, but to a varying degree. The land use/land cover, bioclimatic, edaphic and population groups are associated with globally high R^2 scores, and received a significant boost when adding spatial context, with a large relative increase in performance from 0.47 to 0.61 (+30%) for bioclimatic variables and from 0.40 to 0.54 (+35%) for the edaphic group. The overall highest R^2 scores are obtained for the Vegetation group, both with (0.75) and without (0.74) spatial context, while this small relative improvement when adding spatial context suggests that features at the origin are sufficient to model this group.

For the remaining groups, *geological* and *hydrological*, the model performance remains low in both scenarios, with only a slight increase with spatial context. These variables are discretised from categorical variables and seem hardly pre-

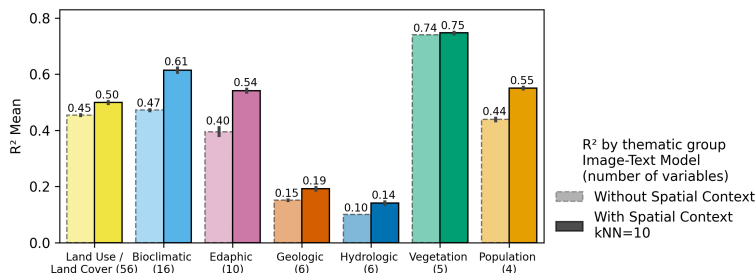


Figure 7: Comparison of model performance on different groups of environmental variables when incorporating spatial context with 10 neighbours. The black line over each bar indicates the standard deviation across five random seeds.

dictable from the RS perspective; adding context information only provides a moderate benefit.

Fig. 8 compares the different settings per group of environmental variables. Overall, the “Text + Images” setting with spatial context performs the best, closely followed by the “Image only” setting, although the gap varies across groups. This confirms a complementary effect from combining modalities, meaning that fusing information from textual and visual data provides a more robust predictive model than either modality alone. The overall weakest performance is obtained again for the geological and hydrological groups, showing a neutral or even negative effect when adding text, which we interpret as the absence of sufficient information for modelling them in the text data.

For vegetation, we observe that using a single image (“Image only”, without spatial context) performs remarkably well, with almost no improvement from either adding text or context, which indicates that these variables are essentially captured by the visual features at the origin.

Clear improvement from “Text + Images” over the next best single modality (“Image only”) is observed for land use/land cover, bioclimatic, population and edaphic variables, suggesting the textual data is most beneficial in these domains. Characteristics describing these variables are more consistently mentioned in textual descriptions of species’ habitat preferences. The presence of useful information is also shown with the relatively strong performance of the “Text only” model for the edaphic and bioclimatic groups. However, the population and land use/land cover variables benefit from incorporating text data only when combined with spatial context.

3.3. Ablation studies

The ablation studies compare several methods to integrate text and location information in the proposed pipeline.

3.3.1. Integrating text

We investigate how to best integrate information from multiple text snippets in our pipeline. We compare three strategies for selecting textual data.

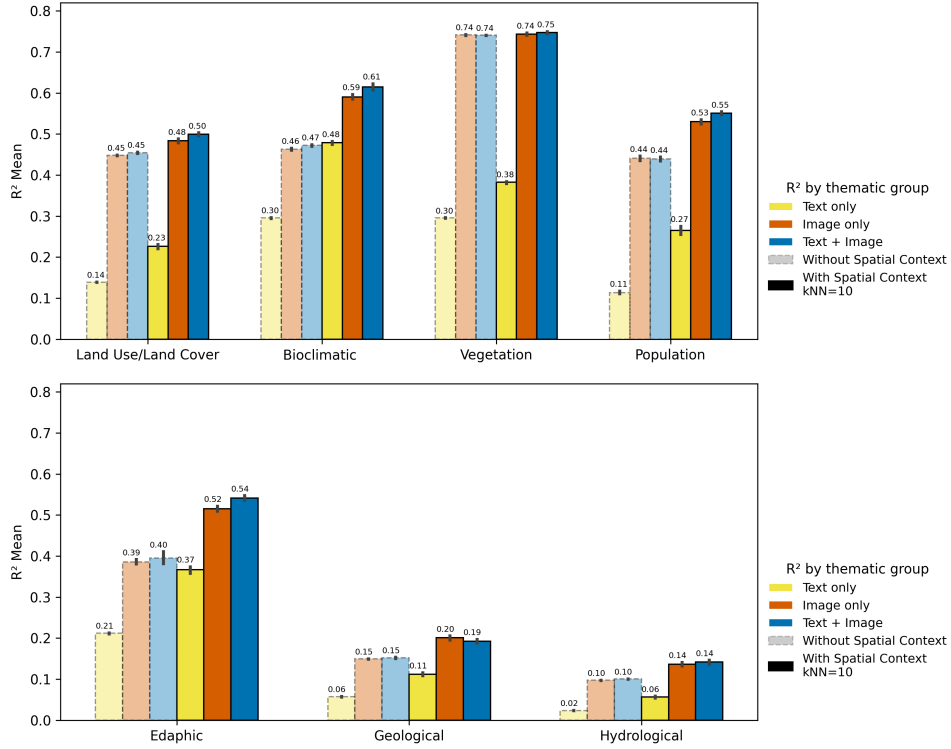


Figure 8: Comparison of performance for the groups of environmental variables when incorporating different modalities with or without spatial context. The black line over each bar indicates the standard deviation across five random seeds.

First, we increase the number of sentences per location by randomly choosing $j \in [0, 1, 2, 4, 8, 16]$ sentences from the location of interest. As the second step, instead of using randomly selected sentences, we choose the top- j with $j \in [0, 1, 2, 4]$ sentences at the location of interest based on the text-image cosine similarity. This ensures that the textual information is aligned with the visual content, acting like a relevance filter of the input text snippets. Finally, we incorporate top- j sentences from NN.

Fig. 9 (a) illustrates the results for the “Text only” setting. More sentences lead to an increase in the R^2 correlation coefficient from 0.10 to 0.15, as the models better capture relevant context, improving the overall results. Selecting a small number of informative sentences (top- j) is more effective than simply increasing the number of sentences for a given location. For instance, selecting the top-4 sentences leads to an R^2 value of 0.17 compared to 0.13 when randomly sampling 4 sentences. When incorporating top- j sentences from NN, the performance climbs to 0.27. For the “Text + Images” model in Fig. 9 (b), we do not see a significant increase in performance between selecting top- j sentences or random sentences, probably due to the fact that the performance is driven

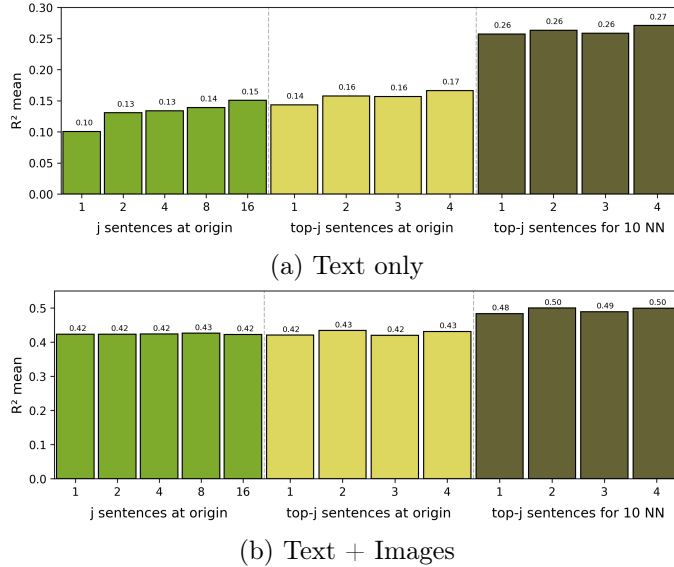


Figure 9: Performance for predicting SWECO25 for (a) the “Text only” model, (b) “Text + Images” model, as correlation coefficient (R^2) for different numbers of sentences per location, and selecting top- j sentences per location based on “Text + 1 Image” cosine similarity with or without integrating a spatial context of 10NN.

mostly by the visual modality and incorporating one or several sentences does not add complementary information. However, similar to “Text only” setting, integrating text from spatial neighbours leads to the overall best performance.

The word clouds in Fig. 10 allow us to grasp qualitatively the effects of selecting top- j sentences based on similarity to the image against random sentences. The clouds are obtained with the *wordcloud* Python library after filtering stop-words, i.e. commonly used words considered insignificant, such as “the”, “and”, and “is”, and grouping sentences according to the ecosystem categories from EcoWikiRS. Filtering the top-1 sentences from the habitat section based on text-image similarity helps to extract objects and concepts related to land cover, and correctly describe the given EUNIS category, except for “low density buildings” category, where few relevant concepts are found. The relevance of the words highlighted quickly degrades when moving to random sentences, where words describing species, i.e. “eagle”, “nest”, “male”, but not their living environment, occur frequently.

3.3.2. Integrating location

This section compares the performances for the different location encoding strategies described in Section 2.3. We examine whether using absolute or relative coordinates is equivalent and whether encoding the distance or the rank to the point of interest is sufficient. Results are presented in Fig. 11.

The “Text only” and the “Text + 1 Image” settings do not exhibit significant

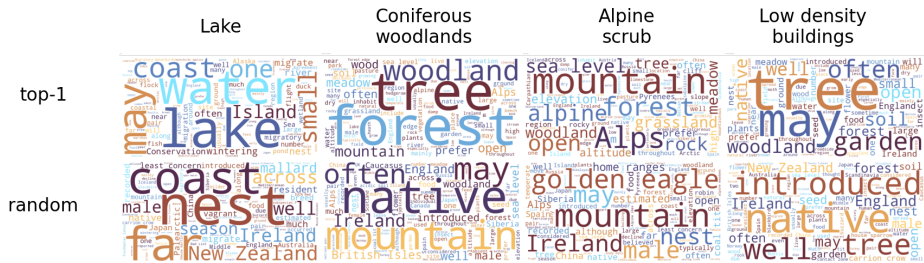


Figure 10: Word clouds illustrating sentences associated with different EUNIS habitats from the EcoWikiRS dataset (rows) and comparison between text selection with top-j or random sentences. Colours serve only to improve readability.

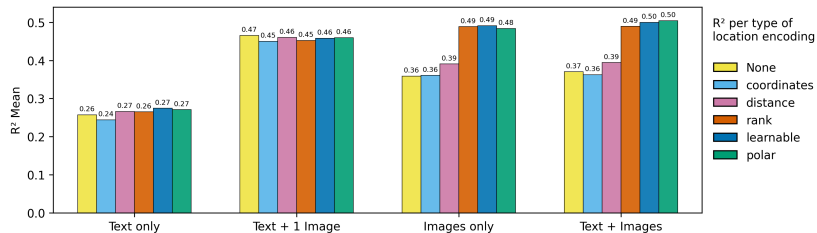


Figure 11: Comparison of different location encoding methods for each model as R^2 score with spatial context ($k=10$).

differences between the different location encoding approaches, while settings involving visual neighbours (“Text + Images”, “Image Only”) show some clear variations. One hypothesis for the absence of improvement when adding location with text is that text encodes information valid over a broad area and not specific to a location, which is potentially redundant to the location encoding, and thus does not help performance.

In the presence of visual neighbours, adding absolute seems not to provide any advantage with respect to adding no location information at all (*None*). As *coordinates* offers a spatial resolution of approximately 1 km when compressed into 512 *dimensions*, it is possibly too coarse for the considered task, with the 10th NN lying at 1 km on average (Suppl. Fig. 13).

We can see better performances with approaches that encode the relative position of NN to the origin location. The *distance* performs only slightly better than *None*, since absolute distance fails to separate neighbours located at similar ranges, but in different directions. *Polar* and *rank* obtain the best performance together with *learnable*. *Rank* and *learnable*, seem to be effective because they order NN by decreasing order of spatial correlation, thus theoretically of decreasing importance. *Polar* encoding is more effective at encoding the spatial context than *distances*: it provides roughly 40 m resolution for distances up to 10 km, and the angle resolves neighbours located at similar ranges but in different directions. Overall, *Polar* obtains similar or best performance, but with fewer trainable parameters, motivating our choice for other experiments.

4. Discussion and Conclusion

Text appears as an emerging modality in geospatial ecology tasks, giving insights into properties hidden from other traditional data sources. However, the fields of application for which text can contribute are not well defined yet, and its combination with other geospatial data sources is limited by its sparse, irregular, and weakly geolocated nature.

This work addresses these issues in two complementary ways. First, we propose a model architecture combining continuous (imagery) and point-based (text) observations: We incorporate all samples in the vicinity of the point of interest, and preserve their spatial structure with a location encoding approach. Second, we provide a quantitative and qualitative study of how text benefits model performance when combined with RS imagery. We evaluate our approach for predicting 103 environmental variables from SWECO25 (Külling et al., 2024) by relying on the EcoWikiRS dataset (Zermatten et al., 2025), composed of aerial imagery and text extracted from Wikipedia, that describes the local environmental context over the Swiss territory.

With respect to the literature, Space2Vec (Mai et al., 2020) is probably the work most similar to our approach, which proposes various spatial encoding methods to classify images associated with their geolocation and their spatial neighbours, and uses an attention-based module to combine the input variables. Similarly to Kriging, Space2Vec integrates target values from the nearest neighbours as predictors in their model, which are not included in our model. Another difference to their approach is that we combine features coming from different modalities (text and images), whereas they focus on tabular data only. Our model also shows some similarities with (Lange et al., 2025), which combines several pairs of geographic coordinates for estimating species ranges, with an attention-based fusion module. The main difference to our work is that they consider geographic coordinates to be the main inputs, and a text, such as species descriptions or pictures are seen as optional metadata.

Our results demonstrated that combining text with RS imagery beats approaches relying only on one individual modality, i.e. "Text only" or "Image only" approach. Moreover, the proposed integration of spatial neighbours consistently provides an additional gain in performance, underlining the benefits of incorporating spatial information for modelling geospatial processes. Text is most beneficial for variables governed by broad-scale processes (climate, edaphic, population), while variables driven by local features (vegetation) remain dominated by imagery. Variables that were poorly predicted from remote sensing alone (e.g., geological and hydrological variables) exhibit a marginal gain from spatial context, and no clear benefit from text integration, suggesting that insufficient relevant information was found in the text data.

Despite promising results, this work presents several potential limitations. First, the scale of the study is limited to Switzerland. While some text-image datasets cover the entire Earth (Daroya et al., 2025), no dataset similar to SWECO25 exists at a global scale with a sufficient spatial resolution, to the best knowledge of the authors, limiting the potential to evaluate such an approach

at the global scale. Second, our experiments only evaluate exploiting Wikipedia articles in English. Extending to multilingual settings and additional textual resources beyond Wikipedia could improve coverage and robustness. Finally, the risk of spatial overfitting cannot be excluded, particularly whether specific “prototype” words dominate predictions at certain locations and how this affects generalisation. Despite the spatial block split, the model may learn spurious correlations and sampling biases rather than true semantic content, an issue difficult to quantify in experimental settings.

Overall, this work demonstrates that sparse, weakly geolocated text can reliably improve spatial regression of environmental variables when integrated through an explicit spatial context model. We hope this work encourages further integration of knowledge from more diverse resources for various applications at the global scale.

Conflict of interest

The authors declare no conflict of interest.

Data Availability

The EcoWikiRS dataset is available at <https://doi.org/10.5281/zenodo.15236742>.

The SWECO25 variables are available at <https://zenodo.org/communities/sweco25/>.

References

- Abdelwahed, H.R., Teng, M., Zbinden, R., Pollock, L., Larochelle, H., Tuia, D., Rolnick, D., 2025. Ciso: Species distribution modeling conditioned on incomplete species observations. arXiv preprint arXiv:2508.06704 .
- Appleby, G., Liu, L., Liu, L.P., 2020. Kriging Convolutional Networks. Proceedings of the AAAI Conference on Artificial Intelligence 34, 3187–3194. doi:[10.1609/aaai.v34i04.5716](https://doi.org/10.1609/aaai.v34i04.5716). number: 04.
- de Arruda, H.F., Reia, S.M., Ruan, S., Atwal, K.S., Kavak, H., Anderson, T., Pfoser, D., 2024. Extracting the U.S. building types from OpenStreetMap data. arxiv.org doi:[2409.05692](https://doi.org/2409.05692).
- Castro, A., Pinto, J., Reino, L., Pipek, P., Capinha, C., 2024. Large language models overcome the challenges of unstructured text data in ecology. Ecological Informatics 82, 102742. doi:[10.1016/j.ecoinf.2024.102742](https://doi.org/10.1016/j.ecoinf.2024.102742).
- Cavender-Bares, J., Schneider, F.D., Santos, M.J., Armstrong, A., Carnaval, A., Dahlin, K.M., Fatoyinbo, L., Hurtt, G.C., Schimel, D., Townsend, P.A., Ustin, S.L., Wang, Z., Wilson, A.M., 2022. Integrating remote sensing with ecology and evolution to advance biodiversity conservation. Nature Ecology & Evolution 6, 506–519. doi:[10.1038/s41559-022-01702-5](https://doi.org/10.1038/s41559-022-01702-5).
- Chen, K., Liu, E., Deng, M., Tan, X., Wang, J., Shi, Y., Wang, Z., 2024. DKNN: deep kriging neural network for interpretable geospatial interpolation. International Journal of Geographical Information Science 38, 1486–1530. doi:[10.1080/13658816.2024.2347316](https://doi.org/10.1080/13658816.2024.2347316).
- Chu, G., Potetz, B., Wang, W., Howard, A., Song, Y., Brucher, F., Leung, T., Adam, H., 2019. Geo-aware networks for fine-grained recognition, in: Proceedings of the IEEE/CVF International Conference on Computer Vision Workshops, pp. 0–0.
- Cole, E., Van Horn, G., Lange, C., Shepard, A., Leary, P., Perona, P., Loarie, S., Mac Aodha, O., 2023. Spatial implicit neural representations for global-scale species mapping, in: International Conference on Machine Learning, PMLR. pp. 6320–6342.
- Cressie, N., 1990. The origins of kriging. Mathematical Geology 22, 239–252. doi:[10.1007/BF00889887](https://doi.org/10.1007/BF00889887).
- Daroya, R., Cole, E., Mac Aodha, O., Van Horn, G., Maji, S., 2025. Wildsat: Learning satellite image representations from wildlife observations, in: Proceedings of the IEEE/CVF International Conference on Computer Vision, pp. 6143–6154.
- Deneu, B., Joly, A., Bonnet, P., Servajean, M., Munoz, F., 2022. Very High Resolution Species Distribution Modeling Based on Remote Sensing

- Imagery: How to Capture Fine-Grained and Large-Scale Vegetation Ecology With Convolutional Neural Networks? *Frontiers in Plant Science* 13. doi:[10.3389/fpls.2022.839279](https://doi.org/10.3389/fpls.2022.839279).
- Derungs, C., Purves, R.S., 2014. From text to landscape: locating, identifying and mapping the use of landscape features in a swiss alpine corpus. *International Journal of Geographical Information Science* 28, 1272–1293. doi:[10.1080/13658816.2013.772184](https://doi.org/10.1080/13658816.2013.772184).
- Domazetoski, V., Kreft, H., Bestova, H., Wieder, P., Koynov, R., Zarei, A., Weigelt, P., 2023. Using natural language processing to extract plant functional traits from unstructured text. *bioRxiv* , 2023–11doi:[10.1101/2023.11.06.565787](https://doi.org/10.1101/2023.11.06.565787).
- Dorm, F., Millard, J., Purves, D., Harfoot, M., Aodha, O.M., 2025. Large language models possess some ecological knowledge, but how much? doi:[10.1101/2025.02.10.637097](https://doi.org/10.1101/2025.02.10.637097).
- Dufour, N., Kalogeiton, V., Picard, D., Landrieu, L., 2025. Around the world in 80 timesteps: A generative approach to global visual geolocation, in: *Proceedings of the IEEE/CVF Conference on Computer Vision and Pattern Recognition*, pp. 23016–23026.
- Fonte, C., Minghini, M., Antoniou, V., Patriarca, J., See, L., 2018. Classification of building function using available sources of vgi. *ISPRS-International Archives of the Photogrammetry, Remote Sensing and Spatial Information Sciences* 42, 209–215. doi:[10.5194/isprs-archives-XLII-4-209-2018](https://doi.org/10.5194/isprs-archives-XLII-4-209-2018).
- Fotheringham, A.S., Brunson, C., Charlton, M., 2009. Geographically weighted regression. *The Sage handbook of spatial analysis* 1, 243–254.
- Gabeff, V., Rußwurm, M., Tuia, D., Mathis, A., 2024. Wildclip: Scene and animal attribute retrieval from camera trap data with domain-adapted vision-language models. *International Journal of Computer Vision* 132, 3770–3786. doi:[10.1007/s11263-024-02026-6](https://doi.org/10.1007/s11263-024-02026-6).
- Gu, J., Stevens, S., Campolongo, E.G., Thompson, M.J., Zhang, N., Wu, J., Kopanav, A., Mai, Z., White, A.E., Balhoff, J., Dahdul, W., Rubenstein, D., Lapp, H., Berger-Wolf, T., Chao, W.L., Su, Y., 2025. BioCLIP 2: Emergent Properties from Scaling Hierarchical Contrastive Learning. doi:[10.48550/arXiv.2505.23883](https://doi.org/10.48550/arXiv.2505.23883). arXiv:2505.23883 [cs].
- Häberle, M., Hoffmann, E.J., Zhu, X.X., 2022. Can linguistic features extracted from geo-referenced tweets help building function classification in remote sensing? *ISPRS Journal of Photogrammetry and Remote Sensing* 188, 255–268. doi:[10.1016/j.isprsjprs.2022.04.006](https://doi.org/10.1016/j.isprsjprs.2022.04.006).
- Hamilton, M., Lange, C., Cole, E., Shepard, A., Heinrich, S., Mac Aodha, O., Van Horn, G., Maji, S., 2024. Combining Observational Data and Language

- for Species Range Estimation. *Advances in Neural Information Processing Systems* 37, 17719–17742.
- Hart, A.G., Carpenter, W.S., Hlustik-Smith, E., Reed, M., Goodenough, A.E., 2018. Testing the potential of twitter mining methods for data acquisition: Evaluating novel opportunities for ecological research in multiple taxa. *Methods in Ecology and Evolution* 9, 2194–2205. doi:[10.1111/2041-210X.13063](https://doi.org/10.1111/2041-210X.13063).
- Kattenborn, T., Schiefer, F., Frey, J., Feilhauer, H., Mahecha, M.D., Dormann, C.F., 2022. Spatially autocorrelated training and validation samples inflate performance assessment of convolutional neural networks. *ISPRS Open Journal of Photogrammetry and Remote Sensing* 5, 100018. doi:[10.1016/j.jphoto.2022.100018](https://doi.org/10.1016/j.jphoto.2022.100018).
- Klemmer, K., Rolf, E., Robinson, C., Mackey, L., Rufswurm, M., 2025a. Satclip: Global, general-purpose location embeddings with satellite imagery, in: *Proceedings of the AAAI Conference on Artificial Intelligence*, pp. 4347–4355.
- Klemmer, K., Rolf, E., Russwurm, M., Camps-Valls, G., Czerkawski, M., Ermon, S., Francis, A., Jacobs, N., Kerner, H.R., Mackey, L., et al., 2025b. Earth embeddings: Towards ai-centric representations of our planet. *Earth-ArXiv preprint* doi:[10.31223/X5HX9S](https://doi.org/10.31223/X5HX9S) doi:[10.1609/aaai.v39i4.32457](https://doi.org/10.1609/aaai.v39i4.32457).
- Külling, N., Adde, A., Fopp, F., Schweiger, A.K., Broennimann, O., Rey, P.L., Giuliani, G., Goicolea, T., Petitpierre, B., Zimmermann, N.E., et al., 2024. Sweco25: a cross-thematic raster database for ecological research in switzerland. *Scientific Data* 11, 21. doi:[10.5281/zenodo.7981110](https://doi.org/10.5281/zenodo.7981110).
- Lang, N., Jetz, W., Schindler, K., Wegner, J.D., 2023. A high-resolution canopy height model of the earth. *Nature Ecology & Evolution* 7, 1778–1789. doi:[10.1038/s41559-023-02206-6](https://doi.org/10.1038/s41559-023-02206-6).
- Lange, C., Hamilton, M., Cole, E., Shepard, A., Heinrich, S., Zhu, A., Maji, S., Van Horn, G., Mac Aodha, O., 2025. Feedforward few-shot species range estimation, in: *International Conference on Machine Learning*, PMLR. p. 0. doi:[10.48550/arXiv.2506.XXXXX](https://doi.org/10.48550/arXiv.2506.XXXXX).
- Liu, W., Chen, J., Wang, H., Fu, Z., Peijnenburg, W.J., Hong, H., 2024. Perspectives on advancing multimodal learning in environmental science and engineering studies. *Environmental Science & Technology* 58, 16690–16703. doi:[10.1021/acs.est.4c03088](https://doi.org/10.1021/acs.est.4c03088).
- Loshchilov, I., Hutter, F., 2019. Decoupled weight decay regularization, in: *International Conference on Learning Representations*, p. 5. doi:arxiv.org/abs/1711.05101v3.
- Mac Aodha, O., Cole, E., Perona, P., 2019. Presence-only geographical priors for fine-grained image classification, in: *Proceedings of the IEEE/CVF International Conference on Computer Vision*, pp. 9596–9606.

- Mai, G., Janowicz, K., Yan, B., Zhu, R., Cai, L., Lao, N., 2020. Multi-scale representation learning for spatial feature distributions using grid cells, in: International Conference on Learning Representations, p. 0.
- Mai, G., Lao, N., He, Y., Song, J., Ermon, S., 2023. Csp: Self-supervised contrastive spatial pre-training for geospatial-visual representations, in: International Conference on Machine Learning, PMLR. pp. 23498–23515. doi:[10.5555/3618408.3619389](https://doi.org/10.5555/3618408.3619389).
- Marcos, D., van de Vlasakker, R., Athanasiadis, I.N., Bonnet, P., Goëau, H., Joly, A., Kissling, W.D., Leblanc, C., van Proosdij, A.S., Panousis, K.P., 2025. Fully automatic extraction of morphological traits from the web: Utopia or reality? Applications in Plant Sciences , e70005.
- Metzger, N., Vargas-Muñoz, J.E., Daudt, R.C., Kellenberger, B., Whelan, T.T.T., Ofli, F., Imran, M., Schindler, K., Tuia, D., 2022. Fine-grained population mapping from coarse census counts and open geodata. Scientific Reports 12, 20085. doi:[10.1038/s41598-022-24495-w](https://doi.org/10.1038/s41598-022-24495-w).
- Miao, Z., Zhang, Y., Fabian, Z., Celis, A.H., Beery, S., Li, C., Liu, Z., Gupta, A., Nasir, M., Li, W., Holmberg, J., Palmer, M., Gaynor, K., Borges, E., Stempel, L., Dodhia, R., Ferres, J.L., 2024. New frontiers in AI for biodiversity research and conservation with multimodal language models. Publisher: EcoEvoRxiv.
- Miłodrowski, R., Extavour, C.G., Ylla, G., 2025. Social media posts as a source of ecological information over time: using twitter (x) as a proof of principle. bioRxiv doi:[10.1101/2025.11.21.689797](https://doi.org/10.1101/2025.11.21.689797).
- Paolo, F.S., Kroodsma, D., Raynor, J., Hochberg, T., Davis, P., Cleary, J., Marsaglia, L., Orofino, S., Thomas, C., Halpin, P., 2024. Satellite mapping reveals extensive industrial activity at sea. Nature 625, 85–91. doi:[10.1038/s41586-023-06825-8](https://doi.org/10.1038/s41586-023-06825-8).
- Paz-Argaman, T., Tsarfaty, R., Chechik, G., Atzmon, Y., 2020. Zest: Zero-shot learning from text descriptions using textual similarity and visual summarization, in: Findings of the Association for Computational Linguistics: EMNLP 2020, pp. 569–579.
- Radford, A., Kim, J.W., Hallacy, C., Ramesh, A., Goh, G., Agarwal, S., Sastry, G., Askell, A., Mishkin, P., Clark, J., Krueger, G., Sutskever, I., 2021. Learning transferable visual models from natural language supervision, in: Meila, M., Zhang, T. (Eds.), International Conference on Machine Learning, PMLR. pp. 8748–8763.
- Rufswurm, M., Klemmer, K., Rolf, E., Zbinden, R., Tuia, D., 2024. Geographic location encoding with spherical harmonics and sinusoidal representation networks, in: International Conference on Learning Representations, p. 5.

- Sathianarayanan, M., Hsu, P.H., Chang, C.C., 2024. Extracting disaster location identification from social media images using deep learning. *International Journal of Disaster Risk Reduction* 104, 104352. doi:[10.1016/j.ijdr.2024.104352](https://doi.org/10.1016/j.ijdr.2024.104352).
- Stevens, S., Wu, J., Thompson, M.J., Campolongo, E.G., Song, C.H., Carlyn, D.E., Dong, L., Dahdul, W.M., Stewart, C., Berger-Wolf, T., et al., 2024. Bioclip: A vision foundation model for the tree of life, in: *Proceedings of the IEEE/CVF Conference on Computer Vision and Pattern Recognition*, pp. 19412–19424.
- Stock, K., Jones, C.B., Russell, S., Radke, M., Das, P., Aflaki, N., 2022. Detecting geospatial location descriptions in natural language text. *International Journal of Geographical Information Science* 36, 547–584. doi:[10.1080/13658816.2021.1987441](https://doi.org/10.1080/13658816.2021.1987441).
- Stringham, O.C., Moncayo, S., Hill, K.G., Toomes, A., Mitchell, L., Ross, J.V., Cassey, P., 2021. Text classification to streamline online wildlife trade analyses. *Plos one* 16, e0254007. doi:[10.1371/journal.pone.0254007](https://doi.org/10.1371/journal.pone.0254007).
- Sun, X., Zhang, Y., Shi, K., Zhang, Y., Li, N., Wang, W., Huang, X., Qin, B., 2022. Monitoring water quality using proximal remote sensing technology. *Science of the Total Environment* 803, 149805. doi:[10.1016/j.scitotenv.2021.149805](https://doi.org/10.1016/j.scitotenv.2021.149805).
- Uzkent, B., Sheehan, E., Meng, C., Tang, Z., Burke, M., Lobell, D., Ermon, S., 2019. Learning to interpret satellite images in global scale using wikipedia. *arXiv preprint arXiv:1905.02506*.
- Vaswani, A., Shazeer, N., Parmar, N., Uszkoreit, J., Jones, L., Gomez, A.N., Kaiser, Ł., Polosukhin, I., 2017. Attention is all you need. *Advances in Neural Information Processing Systems* 30.
- Vendrow, E., Pantazis, O., Shepard, A., Brostow, G., Jones, K., Mac Aodha, O., Beery, S., Van Horn, G., 2024. Inquire: A natural world text-to-image retrieval benchmark. *Advances in Neural Information Processing Systems* 37, 126500–126514.
- Waltari, E., Schroeder, R., McDonald, K., Anderson, R.P., Carnaval, A., 2014. Bioclimatic variables derived from remote sensing: Assessment and application for species distribution modelling. *Methods in Ecology and Evolution* 5, 1033–1042. doi:[10.1111/2041-210X.12264](https://doi.org/10.1111/2041-210X.12264).
- Wang, Q., Ni, J., Tenhunen, J., 2005. Application of a geographically-weighted regression analysis to estimate net primary production of chinese forest ecosystems. *Global Ecology and Biogeography* 14, 379–393. doi:[10.1111/j.1466-822X.2005.00153.x](https://doi.org/10.1111/j.1466-822X.2005.00153.x).

- Wang, R., Gamon, J.A., 2019. Remote sensing of terrestrial plant biodiversity. *Remote Sensing of Environment* 231, 111218. doi:[10.1016/j.rse.2019.111218](https://doi.org/10.1016/j.rse.2019.111218).
- Wang, Z., Prabha, R., Huang, T., Wu, J., Rajagopal, R., 2024. Skyscript: A large and semantically diverse vision-language dataset for remote sensing, in: *Proceedings of the AAAI Conference on Artificial Intelligence*, pp. 5805–5813.
- Wen, S., Zhao, W., Ji, F., Peng, R., Zhang, L., Wang, Q., 2025. “Phenology description is all you need!” mapping unknown crop types with remote sensing time-series and LLM generated text alignment. *ISPRS Journal of Photogrammetry and Remote Sensing* 228, 141–165. doi:[10.1016/j.isprsjprs.2025.07.002](https://doi.org/10.1016/j.isprsjprs.2025.07.002).
- Wolf, S., Mahecha, M.D., Sabatini, F.M., Wirth, C., Bruelheide, H., Kattge, J., Moreno Martínez, Á., Mora, K., Kattenborn, T., 2022. Citizen science plant observations encode global trait patterns. *Nature ecology & evolution* 6, 1850–1859. doi:[10.1038/s41559-022-01904-x](https://doi.org/10.1038/s41559-022-01904-x).
- Xue, X., Zhu, X.X., 2025. Regression in earth observation: Are vision–language models up to the challenge? *IEEE Geoscience and Remote Sensing Magazine* , 2–31doi:[10.1109/MGRS.2025.3596243](https://doi.org/10.1109/MGRS.2025.3596243).
- Yang, T., Xie, J., Li, G., Zhang, L., Mou, N., Wang, H., Zhang, X., Wang, X., 2022. Extracting disaster-related location information through social media to assist remote sensing for disaster analysis: The case of the flood disaster in the yangtze river basin in china in 2020. *Remote Sensing* 14, 1199. doi:[10.3390/rs14051199](https://doi.org/10.3390/rs14051199).
- Zbinden, R., Van Tiel, N., Sumbul, G., Vanalli, C., Kellenberger, B., Tuia, D., 2025. Masksdm with shapley values to improve flexibility, robustness and explainability in species distribution modelling. *Methods in Ecology and Evolution* doi:[0.1111/2041-210X.70200](https://doi.org/0.1111/2041-210X.70200).
- Zermatten, V., Castillo-Navarro, J., Jain, P., Tuia, D., Marcos, D., 2025. Ecowikirs: Learning ecological representation of satellite images from weak supervision with species observations and wikipedia, in: *Proceedings of the Computer Vision and Pattern Recognition Conference*, pp. 2275–2285.

Supplementary Material

4.1. Spatial statistics of the EcoWikiRS dataset

Fig. 12 shows the mean distance to nearest neighbours for samples from the EcoWikiRS train set. Fig. 13 shows the image-to-image and text-to-text cosine similarity as a function of distance for samples from the EcoWikiRS train set, encoded with the SkyCLIP model.

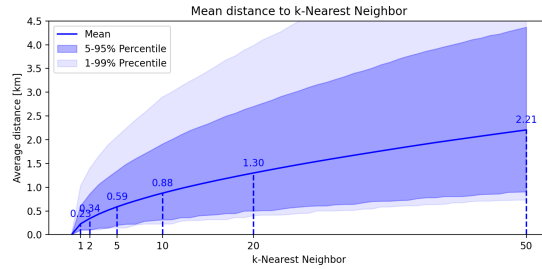


Figure 12: Mean distance to k^{th} nearest neighbours for samples from the EcoWikiRS dataset, with mean and distribution for 5 – 95 and 1 – 99 percentiles.

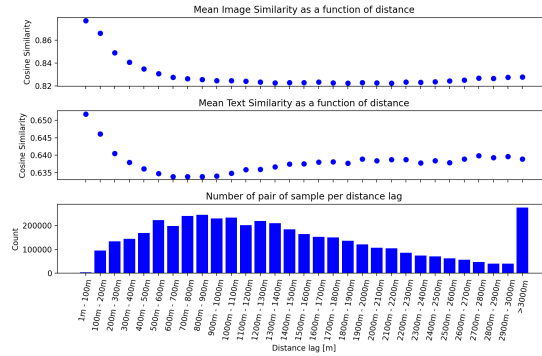


Figure 13: Cosine similarity between image features (a) and text features (b) as a function of the distance between the origin and the NN samples and separated into distance lag of 100m. (c) Number of pairs of samples used to compute the similarity plots above. All values have been computed on the training set of the EcoWikiRS dataset. The horizontal axis is shared among the three plots.

4.2. Additional results

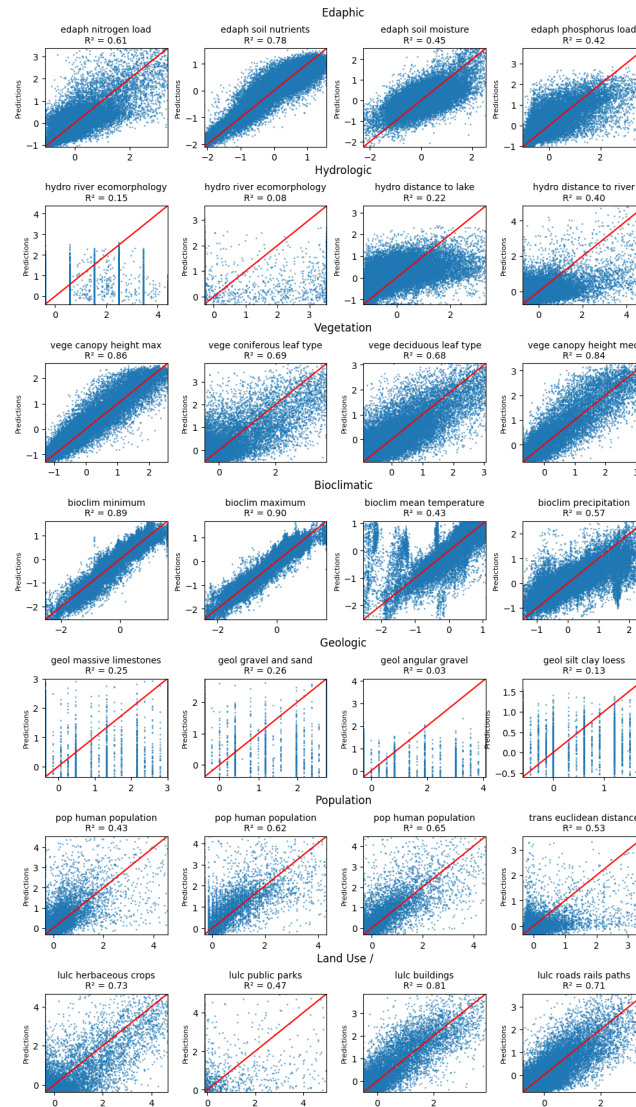


Figure 14: Scatter plots of SWECO25 variables and their predicted values. Four variables per thematic group are randomly plotted. The red line represents the $x = y$ line. Predicted values between 1% and 99% percentiles are plotted (excluding outliers for readability reasons).

Box 4.3 : SWECO layer selection

- bioclim: sub period: 1981 2010.
- edaph: focal: 100.
- lulc: sub period:2023-2018 and focal: 100 or False.
- pop: dataset: wslhabmap and focal: 100 or False, dataset: geostat and sub period: 2020 and focal: 100 or False.
- geol: focal False.
- remote sensing: not included, since we use imagery.
- hydro: dataset: gwn07 and attribute: all, dataset: morph and focal: 100 or False.
- trans: variable long: euclidean distance to roads and attribute: all
- vege: dataset Copernicus: focal: 100 or False, dataset: nfi and focal: 100 or False.

4.3. SWECO25 variables selection and preprocessing

SWECO25 is a swiss-wide raster database at 25-meter resolution composed of 5'265 layers. All variables are numerical, with categorical variables encoded with a distance buffer (focal) of 100m, if not mentioned otherwise. Some SWECO variables exhibit a strong imbalanced distribution, with most values equal to zero, for example, rare land cover classes. SWECO values are extracted and averaged for each location of the EcoWikiRS dataset, following the footprint of the aerial images. The numerical values are standardised with a zero mean and a unit variance.

A primary selection of 307 variables is arbitrarily made based on the layer descriptions, spatial resolution and their interest potential for regression from EO and text data. This primary selection followed a set of rules shown in the Box 4.3. The final set of 103 SWECO variables is obtained by (1) removing variables with a standard deviation smaller than 0.01, (2) removing duplicate columns, defined by two columns with a correlation superior to 0.98, (3) removing variables with low importance. This last criterion is operated by fitting a random forest model on SWECO variables to predict the EUNIS ecosystem labels from the EcoWikiRS dataset. Features importance are computed for each SWECO variable, and a fraction of 0.5 of variables with the lowest importance is removed, leading to the final set of 103 SWECO variables.

Table 1: SWECO25 variables name and description (unit)

SWECO25 Geology variables	Description (unit)
edaph_eiv_d_25	soil aeration (index (low to high))
edaph_eiv_f_25	soil moisture (index (dry to wet))
edaph_eiv_h_25	soil humus (index (humus poor to rich))
edaph_eiv_k_25	continentality (index (atlantic to continental))
edaph_eiv_l_25	light (index (shaded to sunny))
edaph_eiv_n_25	soil nutrients (index (nutrient poor to rich))
edaph_eiv_r_25	soil ph (index (acidic to alkaline))
edaph_eiv_w_25	soil moisture variability (index (low to high))
edaph_modiffus_n_25	nitrogen load (kilogram per hectare per year)
edaph_modiffus_p_25	phosphorus load (kilogram per hectare per year)
SWECO25 Geology variables	Description (unit)
geol_geotechnic_cl1	lakes cover (percentage cover)
geol_geotechnic_cl19	massive limestones (percentage cover)
geol_geotechnic_cl3	silt, clay, loess, ground moraine, surface moraine (percentage cover)
geol_geotechnic_cl5	gravel and sand (glacial deposit) (percentage cover)
geol_geotechnic_cl6	gravel and sand (current deposit) (percentage cover)
geol_geotechnic_cl7	angular gravel, blocks, slope scree (percentage cover)
SWECO25 Population variables.	Description (unit)
pop_statpop_2020_populationdensity	human population density (number of inhabitants)
pop_statpop_2020_populationdensity_mean_100	human population density (number of inhabitants)
pop_statpop_2020_populationdensity_sum_100	human population density (number of inhabitants)
trans_tlm3d_dist2road_all	euclidean distance to roads (meters)
SWECO25 Vegetation variables.	Description (unit)
vege_copernicus_coniferous_100	coniferous leaf type (percentage cover)
vege_copernicus_deciduous_100	deciduous leaf type (percentage cover)
vege_nfi_canopy_max_100	canopy height (meters)
vege_nfi_canopy_median_100	canopy height (meters)
vege_nfi_canopy_min_100	canopy height (meters)
SWECO25 Hydrologic variables	Description (unit)
hydro_gwn07_dist2lake_all	distance to lake (meters)
hydro_gwn07_dist2riverstrahler_all	distance to river (meters)
hydro_morph_oekomorphology	river ecomorphology (percentage cover)
hydro_morph_oekomorphology_cl1_100	river ecomorphology (percentage cover)
hydro_morph_oekomorphology_cl2_100	river ecomorphology (percentage cover)
hydro_morph_oekomorphology_cl3_100	river ecomorphology (percentage cover)

Table 1: continued from previous page.

SWECO25 Bioclimatic variables	Description (unit)
bioclim_chclim25_present_1981_2010_ai	aridity index (index (dry to wet))
bioclim_chclim25_present_1981_2010_bio15	precipitation seasonality (coefficient of variation)
bioclim_chclim25_present_1981_2010_bio16	precipitation of wettest quarter (millimetre)
bioclim_chclim25_present_1981_2010_bio17	precipitation of driest quarter (millimetre)
bioclim_chclim25_present_1981_2010_bio18	precipitation of warmest quarter (millimetre)
bioclim_chclim25_present_1981_2010_bio19	precipitation of coldest quarter (millimetre)
bioclim_chclim25_present_1981_2010_bio2	mean diurnal range (degree Celsius)
bioclim_chclim25_present_1981_2010_bio3	isothermality (degree Celsius)
bioclim_chclim25_present_1981_2010_bio4	temperature seasonality (degree Celsius)
bioclim_chclim25_present_1981_2010_bio7	temperature annual range (degree Celsius)
bioclim_chclim25_present_1981_2010_bio8	mean temperature of wettest quarter (degree Celsius)
bioclim_chclim25_present_1981_2010_bio9	mean temperature of driest quarter (degree Celsius)
bioclim_chclim25_present_1981_2010_etp	evapotranspiration (millimetre)
bioclim_chclim25_present_1981_2010_prec	precipitation (millimetre)
bioclim_chclim25_present_1981_2010_tmax	maximum temperature (degree Celsius)
bioclim_chclim25_present_1981_2010_tmin	minimum temperature (degree Celsius)

Table 1: continued from previous page

SWECO25 Land Use	Land Cover variables	Description (unit)
lulc_wslhabmap_cl11	100	still water (percentage cover)
lulc_wslhabmap_cl12	100	running water (percentage cover)
lulc_wslhabmap_cl21	100	vegetated shoreline (percentage cover)
lulc_wslhabmap_cl22	100	low marshes (percentage cover)
lulc_wslhabmap_cl32	100	alluvium and moraines (percentage cover)
lulc_wslhabmap_cl33	100	scree (percentage cover)
lulc_wslhabmap_cl34	100	cliffs (percentage cover)
lulc_wslhabmap_cl40	100	grass and artificial meadows (percentage cover)
lulc_wslhabmap_cl41	100	rock slabs and limestone pavement (percentage cover)
lulc_wslhabmap_cl42	100	thermophilic dry grassland (percentage cover)
lulc_wslhabmap_cl43	100	high altitude grasslands and rough pastures (percentage cover)
lulc_wslhabmap_cl45	100	rich meadow (percentage cover)
lulc_wslhabmap_cl52	100	megaphorbs, forestry cuts (percentage cover)
lulc_wslhabmap_cl53	100	bushes and shrubs (percentage cover)
lulc_wslhabmap_cl54	100	heaths (percentage cover)
lulc_wslhabmap_cl60	100	planting (percentage cover)
lulc_wslhabmap_cl62	100	beech forest (percentage cover)
lulc_wslhabmap_cl63	100	other broadleaf forests (percentage cover)
lulc_wslhabmap_cl66	100	highland coniferous forest (percentage cover)
lulc_wslhabmap_cl81	100	woody plant crops (percentage cover)
lulc_wslhabmap_cl82	100	herbaceous crops (percentage cover)
lulc_wslhabmap_cl92	100	buildings (percentage cover)
lulc_wslhabmap_cl93	100	roads, rails, paths (percentage cover)
lulc_wslhabmap_cl94	100	parking, sport grounds (percentage cover)
lulc_wslhabmap_gr1	100	water (percentage cover)
lulc_wslhabmap_gr2	100	shores and wetlands (percentage cover)
lulc_wslhabmap_gr3	100	glaciers, rocks, scree and moraines (percentage cover)
lulc_wslhabmap_gr4	100	grasslands and meadows (percentage cover)
lulc_wslhabmap_gr5	100	heaths, forest edges and megaphorbs (percentage cover)
lulc_wslhabmap_gr6	100	forests (percentage cover)
lulc_wslhabmap_gr7	100	pioneer vegetation in areas disturbed by humans (percentage cover)
lulc_wslhabmap_gr8	100	plantations, fields and crops (percentage cover)
lulc_wslhabmap_gr9	100	built environments (percentage cover)

Table 1: continued from previous page

SWECO25 Land Use	Land Cover variables	Description (unit)
lulc_geostat25_present_2013_2018_cl12	100	surroundings of agricultural buildings (percentage cover)
lulc_geostat25_present_2013_2018_cl14	100	surroundings of unspecified buildings (percentage cover)
lulc_geostat25_present_2013_2018_cl2	100	surroundings of industrial and commercial buildings (percentage cover)
lulc_geostat25_present_2013_2018_cl31	100	public parks (percentage cover)
lulc_geostat25_present_2013_2018_cl32	100	sports facilities (percentage cover)
lulc_geostat25_present_2013_2018_cl39	100	vineyards (percentage cover)
lulc_geostat25_present_2013_2018_cl41	100	arable land (percentage cover)
lulc_geostat25_present_2013_2018_cl42	100	meadows (percentage cover)
lulc_geostat25_present_2013_2018_cl43	100	farm pastures (percentage cover)
lulc_geostat25_present_2013_2018_cl46	100	favorable alpine pastures (percentage cover)
lulc_geostat25_present_2013_2018_cl4	100	surroundings of one- and two-family houses (percentage cover)
lulc_geostat25_present_2013_2018_cl50	100	normal dense forest (percentage cover)
lulc_geostat25_present_2013_2018_cl51	100	forest strips (percentage cover)
lulc_geostat25_present_2013_2018_cl56	100	open forest (on unproductive areas) (percentage cover)
lulc_geostat25_present_2013_2018_cl57	100	brush forest (percentage cover)
lulc_geostat25_present_2013_2018_cl59	100	clusters of trees (on agricultural areas) (percentage cover)
lulc_geostat25_present_2013_2018_cl62	100	rivers (percentage cover)
lulc_geostat25_present_2013_2018_cl65	100	unproductive grass und shrubs (percentage cover)
lulc_geostat25_present_2013_2018_cl67	100	wetlands (percentage cover)
lulc_geostat25_present_2013_2018_cl69	100	rocks (percentage cover)
lulc_geostat25_present_2013_2018_cl70	100	scree, sand (percentage cover)
lulc_geostat25_present_2013_2018_cl8	100	surroundings of blocks of flats (percentage cover)
lulc_geostat25_present_2013_2018_cl10	100	surroundings of public buildings (percentage cover)